

On soot sampling: Considerations when sampling for TEM imaging and differential mobility spectrometer

Emberson DR, Rohani B, Wang PhD L, Sæterli PhD R, Lovas T

Abstract

Particulate matter (PM) has been sampled from a compression ignition engine using a differential mobility spectrometer (Cambustion DMS 500) and for imaging in a transmission electron microscope (TEM) with the aim of coupling these two measuring techniques. A known issue when coupling these two methods is that a device like the DMS samples all PM, and the TEM only soot. To help resolve this issue, a thermal denuder was designed and built to remove all volatile organic compounds (VOC) from the sample prior to entering the DMS. For TEM imaging, soot was either collected directly onto a TEM grid using the thermophoretic effect or collected onto quartz filters with the soot then transferred onto the TEM grids. The direct to grid technique did not work after the denuder due to the gas temperature being too low for the thermophoretic effect; hence the reason to collect some soot using the quartz filters. Soot was removed from the filters using an ethanol wash/sonication technique. Morphology; diameter of gyration, projected area, primary particle size and fractal dimension have been compared between the two TEM sampling techniques, with or without the denuder. Denuder effectiveness has been assessed using TGA analysis of sampled soot. Issues concerning the sampling process itself are outlined. A comparison between the TEM and the DMS results is conducted with the discrepancies between them discussed. Direct and filter sampling gave similar results as long as the sonication process and grid prep is done properly, otherwise the filter wash technique results in a number of clusters of agglomerates which distorts the post processing and morphological data.

Introduction

Soot and PM generated in internal combustion engine (ICE) is harmful to human health and is strictly regulated. Recent emissions problems surrounding the diesel engine have led to soot and PM emissions coming under greater scrutiny from the research community, the engine community and the public at large. Whilst it is essential to mitigate the emissions, it is also true that robust measurement is needed, and the measurement methodologies being applied should also come under scrutiny.

The work presented here details the stages of development of a protocol to sample soot from a fully instrumented engine and later apply this modified protocol to an optically accessible compression ignition combustion chamber (OACIC). The points of interest and findings that have been observed during this development phase have not been adequately discussed in the literature and the authors believe that this study could form the basis of a form of blueprint for future researchers developing an experimental investigation into soot and PM. The work describes an empirical development phase. Although no clear results concerning the science of soot are really presented, there are several points and issues raised that are highly relevant to the engine soot research community.

Soot and particulate matter (PM) are created during combustion. Soot is usually defined as a solid carbonaceous product of combustion whilst PM covers all small particles, irrelevant of source, i.e. there are PM emissions from brake pads during braking of vehicles. Combustion PM covers all particulate that is emitted due to the combustion of a fuel in air. They will include the solid carbonaceous soot (40-50% of the PM by mass, highly dependent on combustion conditions [1, 2]), condensing volatile compounds, sulphur-based compounds, lubricating oil compounds, metals-based compounds.

Engine exhaust gases are therefore a PM laden gas flow. The PM may be sampled *in situ* using a variety of devices (see review article [3]). Basic measurement will often give the total mass of PM that has been emitted within a given time frame or may be calculated to give a specific measure, i.e. g/kWh. This form of measurement will essentially rely on some form of PM capture, often using a filter of some form. This basic measure is referred to as a gravimetric measurement and though insightful can be misleading on the possible impacts of the PM generated as the PM size is not considered. PM size is extremely important. Whilst PM is referred to by a rather broad size categorization of PM₁₀ or PM_{2.5} [4] to give some form of size descriptor to the PM, it should be clear that PM can come in sizes ranging from a few nm up to 1000's nm.

As new legislation comes into force, the particle size distribution is becoming more important. To this end there are numerous devices

used to provide a measure of the particle sizes being emitted [1, 3, 5]. The work presented here has made use of a differential mobility spectrometer (DMS) from Cambustion. The other device that is most likely the most common is a scanning mobility particle sizer (SMPS). Both devices make use of the electrical mobility of a charged particle in an electric field, with the motion of the charged particle dependent on the electrical charge imparted onto the particle and the aerodynamic drag on the particle, both of which are a function of particle size, as well as the electric field applied.

DMS design and operation is described in the works [6, 7]. The measurement is presented as the particle number concentration in terms of $dN/d\log D_p$ with units of N (cc) (number per cubic centimetre). This is a consequence of the log normal distribution of the particulate. dN is the number of particles in the range (total concentration) and $d\log D_p$ is the difference in the log channel width. $d\log D_p$ is determined by subtracting the log of the lower bin boundary from the log of the upper boundary for each channel (normalizing for bin width). The concentration is divided by the bin width, giving a normalized concentration value that is independent of bin width. This allows comparison between machines that may operate with a different resolution.

Defining the size of PM and soot with a single number is required, particularly for legislation purposes, but it does ignore the fact that the soot element of the PM is not spherical, and any single number being used to define its size is missing information. Soot is a complex fractal like structure which appears to be made up of smaller particles that have coalesced and combined to form an aggregate structure. The smaller particles are referred to as primary particles, which form during combustion. As these primary particles collide and combine, soot aggregate particles “grow” [8]. These aggregates have a shape-a *morphology*. The study of soot morphology via imaging of the soot aggregates is well described in the works [9-11]. To understand the soot formation process or the influence of any variables (fuel type, injection strategy, engine operational conditions) on the soot formation process, soot morphology should be examined. Further indication of the soot formation process is gleaned from examination of the primary particles and the graphitic structure of the carbonaceous solids. A common method used for these studies is the imaging of soot in a transmission electron microscope (TEM). With the correct collection methodology applied, soot morphology, soot primary particles and soot graphitic layers can be examined, with image post processing applied to automate the calculations and measurements made from the images of a large number of particles.

The PM admitted into the exhaust gases contains soot which is the product of the competition between the growth of these particles and the oxidation of them. This soot will then have volatiles condensing onto and evaporating from their surface, along with further collisions, wall impaction and dilution with other gases. It is an un-stable situation, the soot sampled will be dependent on the sampling method used, dilution applied, temperatures applied, filters used, lengths and shapes of any tubing used. Dilution of soot sample is a very large issue that needs to be well considered and designed, especially for legislation measurements that need to be general. Due to the nature of the DMS used here, direct from exhaust sampling is used, with the DMS handling dilution, hence it is not discussed in this work.

The combination of a DMS or SMPS (sizer) type measurement with a TEM analysis is rare- with a few examples in the literature [12-14]. In most cases a direct comparison between the two measurements is not made. The work of Seong [14] conducted tests using SMPS and TEM analysis and a discrepancy between the two measurements was put

down to the volatile organic compounds (VOC) that form the nucleation (very small, below 20nm) mode particles that will be measured by a sizer but not observed in the TEM.

The work of Miyashita [13] examined soot in TEM and SMPS with a gasoline engine, this is the only work that the authors have found that attempts to directly combine the two measures in a single analysis. Here the distribution of the size of the particle aggregates, measured in the TEM, defined as the radius of gyration of the particles is plotted along with the distribution from the SMPS.

As a robust protocol to sample soot is being developed, the authors decided to conduct a study examining the measurement of PM and soot made with a DMS and with imaging in a TEM. To this end the authors hypothesized that an analysis could be conducted that would demonstrate a similar distribution of sizes measured by both techniques. In doing so the authors considered the previous works where a ‘sizer’ had been used along with TEM imaging and decided to remove the problem of VOCs condensing onto the surface of soot (changing their size) or forming small particles that the sizer would measure but would not be visible in the TEM.

Distinction between the non-volatile and volatile exhaust PM fractions is required to understand the origin, physical properties, and implications of exhaust aerosol. An aerosol conditioning device, often referred to as volatile particle removers (VPRs) eliminates the volatile aerosol fraction by thermally treating the sample [15]. One such VPR is a thermal denuder. A thermal denuder to remove the VOCs from the sample on route to the sizer was developed.

Though not solely applied to engine combustion PM sampling, thermal denuders have been used by several researchers [15-18]. A thermal denuder consists of a heater section, which heats up the PM laden gas flow to a high enough temperature to ensure all volatiles are in the gas phase. This hot, PM laden gas then flows into an absorber (denuder) section, consisting of an activated carbon, absorbing medium housed around the flow. The carbon is actively cooled, with air or water to set up a thermal gradient which should help drive the evaporated volatiles into the carbon where they are absorbed and removed from the gas flow. The sample then leaves the denuder and enters the DMS or SMPS or filter. The authors postulate that the application of a denuder in conjunction with the DMS will assist in direct comparison between the DMS and TEM measurements. To this end, a thermal denuder was designed and built following the design and suggestions outlined in [19-21].

Whilst the methods so far have all considered size, shape or amount, they have not examined the soot components. Thermal gravimetric analysis (TGA) of soot gives a measure of the volatile organic fraction (VOF) of the soot and can be applied to examine the reactivity of the soot (with oxygen). TGA analysis involves measuring the mass loss of a small sample whilst heated, either in an inert (nitrogen) atmosphere of an oxygenating (oxygen or air) atmosphere. Hence the change in mass indicates the VOF under inert heating and the fraction that can be oxidized (burnt) under oxygenating heating. A small sample of the soot (1-5mg minimum) is required for TGA. For the purpose of developing a complete soot characterization protocol and to examine the effectiveness of the thermal denuder, it was decided to include a TGA study.

To summaries this study: the authors established a desire to sample soot using a DMS and TEM imaging and develop an analysis comparing the two methods. To aid the sampling, a thermal denuder has been incorporated to remove VOC destined for the DMS to aid the

comparison between the DMS and the TEM measurements as it is believed the presence of VOC will change the size distribution measured by the two techniques.

Thermal denuder effectiveness has been examined with a TGA measurement. Implementing the TGA measurement meant a minimum mass of soot needed to be collected. This influenced the engine conditions that were used to ensure an adequate amount of soot was collected in a sensible (around 1 hour) period. A relatively short period of time is desired for collection as the protocol will be used with some fuels in the future that are expensive. Three methods to collect soot have been considered a.) using a cooled glass surface; b.) using a quartz filter; c.) direct to TEM grid.

Soot collection protocol

To develop a robust protocol and investigate the influence of collection methods along with the assessment of the thermal denuder, a fully instrumented engine was used, essentially as a particle generator. The engine is a 6 cylinder; Mercedes OM 613 engine is connected to a hydro-dynamometer from Stuska. The engine is equipped with a 2nd generation Bosch common rail system and installed with a Variable Nozzle Turbocharger. All manufacturer emission devices and controls have been removed from the engine (EGR and catalysis). Engine control is achieved with a Bosch motor sport ECU coupled to Modas software. All engine parameters are user controlled, no manufacturer engine mapping has been used. Dynamometer control, fuel cooling control, test cell conditions and all data logging is achieved with a National Instruments CompactRIO and a LabView program.

Initial testing was concerned with finding a suitable operating condition to conduct tests. Initially the use of a condition that would create a large number of nucleation particle, which would contain a lot of VOCs was considered, this could then be used to test the thermal denuder. However, previous testing in the engine had shown that only at low load conditions are nucleation particles really observed with DMS. Figure 1 shows the DMS data collected from a large test previously conducted, using Diesel fuel and 1st generation biodiesel fuel. It is evident that at the three speeds investigated, only the low load condition of 20Nm (and 50Nm for the low speed) has nucleation mode PM. A compromise at this point was made. It was found that at these low loads, and relatively low speed conditions, the rate of soot creation was low and that the time required to collect enough soot for TGA analysis (5mg was original target) was too long to be a sensible period for an experimental test. The work [22] used an injection quantity of 25mg per injection (single cylinder heavy duty engine) as target which resulted in a high filter smoke number (FSN) which resulted in sensible collection times. A target of 20mg per injection (output from ECU data) at 2000rpm resulting in 140Nm torque (35% max) was used in this study. The compromise was that there were no nucleation particles, which made observing the thermal denuder influence on nucleation particles impossible, something that had been intended during initial developments. There was still VOCs present for the denuder to remove.

Whilst conducting initial tests before the final operating condition had been settled on, with the thermal denuder in mind, conditions resulting in large amounts of nucleation particles were examined, this is shown in Figure 2. The number of peak nucleation particles was found to be sensitive to the exhaust conditions and repeatability was very dependent on the previous state of the engine (temperature in the exhaust system and turbo). The figure shows the DMS data from 1400rpm, 20Nm that has undergone varying loads, speeds and turbo settings prior to collection.

Page 3 of 9

06.06.2019

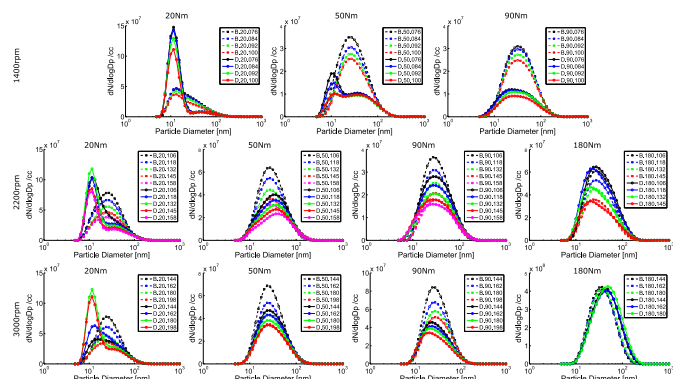


Figure 1. Particle number results from previous test [23] showing change in size distribution with engine speed and torque (load) for diesel and biodiesel.

It is understood that the exhaust system temperature was different for each collection; it can be seen that the nucleation particles are sensitive to this change. As purpose of any test at this condition would be to examine the influence of the denuder on the nucleation particle reduction via VOC adsorption it was another reason not to conduct any testing at this condition.

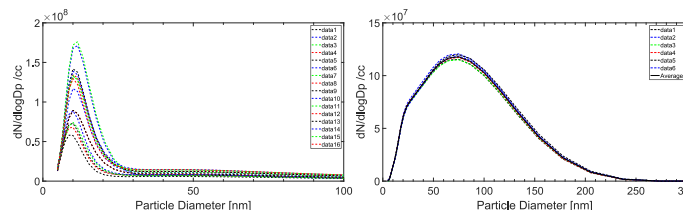


Figure 2. Particle size distribution at low speed, low load (1400rpm, 20Nm) with peak number in nucleation mode size (left) and distribution at the higher speed, higher load condition considered (2000rpm, 140Nm).

A relatively late injection timing of 10 CAD BTDC was chosen that: resulted in a relatively late combustion; maximised VOC in the exhaust and; was found to give high soot. Exhaust temperature was high at around 400°C. This high temperature improved repeatability of measured PM in the DMS and ensured no VOC would condense prior to sampling. Injection pressure was set at 400bar. Figure 3 shows the cylinder pressure and heat release rate for the engine condition used.

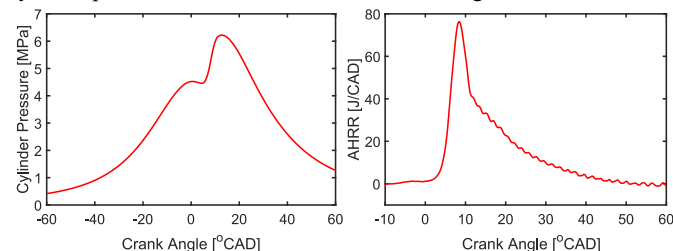


Figure 3. Engine cylinder pressure and heat release rate at 2000rpm, 140Nm, 10 CAD BTDC injection timing.

Thermal denuder

The denuder follows the designs outlined in [19, 21], it is divided into two parts, the heating and the cooling section. In the heating section, VOCs evaporate and desorb from the surface of the soot. In the cooling section, the evaporated particles are absorbed by activated carbon. The heating section of the thermal denuder has a length of 500mm and an inner diameter of 13mm. It is made of a stainless-steel tube and

surrounded with electrical heating tape (Omega, Ultra-High Temperature Heating Tape) which is then wrapped in a fibre glass insulation tape and all sealed in silicone sealing tape (good up to 360°C), see Figure 4. A benchtop PID (OMEGA iSeries) coupled to a K type thermocouple located 250 mm along the heater section controls temperature. The cooling section is 500mm long with a mesh-tube, inner diameter of 20mm, inside of it. The outer diameter is 60mm. The mesh-tube is surrounded by activated carbon, which is cooled by water through a copper coil which ensures a stable temperature in the carbon and improves the absorption of the VOCs. The residence time of the particles is 12.3 s in the heating section and 29 s in the carbon section, determined from the flow velocity of the DMS500 sample line (1.3 l/min). The time in the heating section should be as long as possible [19] with VOC evaporation time depending on the particle composition and diameter. The work [21] states the thermophoretic losses increase and the transmission efficiency decreases with increasing temperature in the heating section, which is caused by the temperature difference between the wall and the gas flow in the cooled adsorber section. Particles will drift from the center of the gas flow because of the lower wall temperature [19]. In case of quantitative measurements with the thermal denuder, the transport efficiency must be used to correct the data- this should be determined experimentally and will be size dependent.

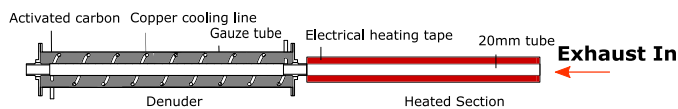


Figure 4. CAD drawing of the thermal denuder.

Figure 5 shows the engine and DMS with and without the denuder. The exhaust temperature where the denuder was attached to the exhaust was approx. 400°C, the denuder heater was set to its maximum of 300°C, cooling water was 20°C. The denuder was held in the horizontal position during sampling. The sampling point is approx. 1 meter from the end of the exhaust manifold, with the manifold and the exhaust insulated up to the sampling point.

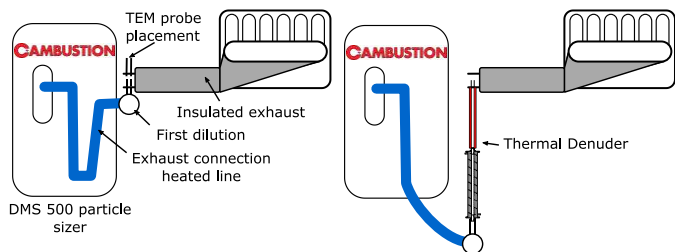


Figure 5. Engine and DMS configurations.

A correction has been applied based on an estimation of the transmission efficiency of the denuder. As the design and operation of the denuder used here is similar to that in the work [21], the size dependent transmission efficiency has been determined from the results published in [21] and used to correct the collected DMS results “With Denuder” in Figure 6. There is a considerable reduction in the number of particles sampled when the denuder is in place. Even with the correction applied, it is not possible to determine if this drop is purely down to VOC removal or particle losses. The fact that the position of the peak size has moved little, and the drop seems quite similar across all sizes, it is suspected that the losses have been higher than expected.

Soot collection

Direct to grid TEM

For the analysis using a TEM, soot was collected on 3mm diameter, 200 mesh, copper grids with continuous carbon nano-film. The continuous carbon is used as this provides a constant background in the TEM images collected, this is essential during the image processing to identify particles from background. Other grids in use are lacey or holey (carbon film) type. These do not have a continuous film but a film with rips or holes. These are used when observing the nano-structure of the soot at much higher magnification. When probing the inner structure of the soot particles, the electron beam must be transmitted through the particle with no grid surface behind it. A holey or lacey type grid makes use of a particle stuck to the film “hanging” over the edge of hole, hence the electron beam passes through particle only.

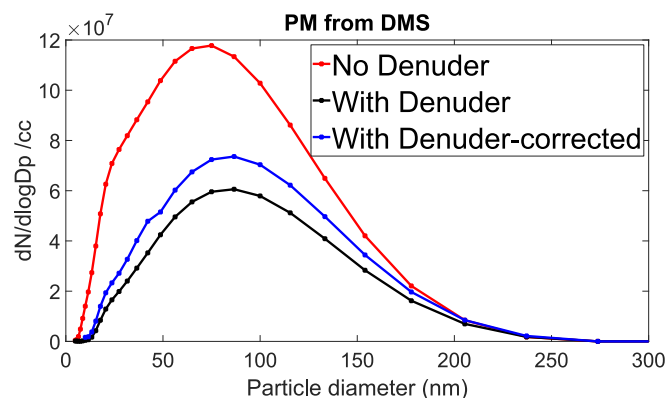


Figure 6. DMS results of PM size distribution direct from the exhaust, no denuder fitted (red), with denuder fitted (black) and with the denuder fitted and a size dependent correction applied, extrapolated from results in [21].

The soot is thermophoretically sampled on the grid using the temperature gradient between the hot exhaust gases and the grid surface. A sampling probe was designed and built that could be used to insert the grid into the exhaust stream through a port in the exhaust. The probe is made from stainless steel, with the grid sitting at the bottom of 2mm diameter hole. The probe provides a good thermal mass to protect the grid and to maintain a thermal gradient between the grid surface and the exhaust gases. Five probes were built to assist with sampling; a sample could be collected, sealed and stored still in the probe before being imaged. Figure 7 shows a drawing of the probe, the red arrow is the gas flow direction.

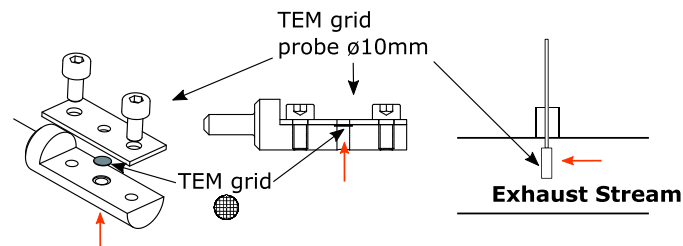


Figure 7. TEM grid probe.

Soot for TEM was sampled direct from the exhaust using the probe (before the denuder) and after the denuder. It was found that after the thermal denuder, the thermophoresis method was not adequate; there was condensation and the temperature gradient was not high enough to drive particles onto the grid. The authors wished to collect soot for

TEM analysis after the denuder to investigate if the soot morphology or primary size was affected by the denuder, so an alternative method was sought. This is discussed in the coming sections.

Different periods of exposure of the grid to the exhaust were examined, ranging from 1 second up to 30 seconds (regular intervals examined). 5 seconds exposure was found to give a good sampled soot area ratio (total area of sampled soot in a single 6000 mag image/total area of image). Typical soot sample area ratio was 10% here, the work [13] reported a value between 1 and 10% to be acceptable. This collection time would be non-transferable to another engine or test situation; it is advised that this step of assessing time of exposure should always be taken. Too long and the grid may be damaged due to heat or overlaid with soot particles, too little and the number of particles captured in one image drops too low, requiring more images to be taken in the TEM, to capture a statistically significant number of particles.

Soot collection for TGA

To collect soot for examination in the TGA (before and after the denuder) soot was collected using a cooled glass surface in a chamber, Figure 8. The cooled glass surface idea came from the work [24]. It had the potential to provide benefits over other bulk collection methods, mainly that the sample could be scraped or washed off without contaminating the sample with filter material, useful for some analysis techniques such as XRD and Raman spectroscopy, where filter fibres would be in any spectrum, superimposed on soot spectrum.

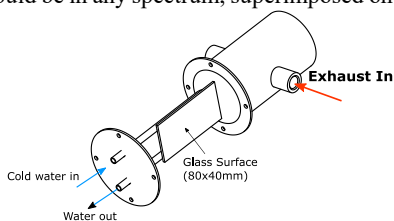


Figure 8. Cooled glass surface soot collector.

The glass surface was 40 by 70mm and secured in a steel tube section, the exhaust sample was drawn over the cooled surface using the DMS as the vacuum, this was done to ensure for all cases through the denuder, residence time was kept constant. The technique was shown to be completely inadequate, requiring extremely long run times to collect 1mg of soot, which had been contaminated with condensing water. After a number of attempts, the technique was no longer considered.



Figure 9. 47mm polycarbonate inline filter holder. Plastic hose spears were replaced with stainless Swagelok items. Filters used were 2500 QAT-UP 47mm.

A filter was then used to collect bulk sample. Common filter materials are Teflon [25] or quartz [26]. The sample must be removed from the filter and prepared for analysis with either the complete removal of the filter material or used in an analysis that is insensitive to the filter material i.e. dissolve the Teflon with dichloromethane; quartz is inert, should not be oxidised in a TGA.

A 47mm quartz filter in a polycarbonate filter holder was fitted in the sampling line before and after the denuder. To avoid over heating when fitted directly to the exhaust before the denuder, a cooling air jet was directed at the outer of the filter inlet. Sample was collected for 30mins using the DMS as the vacuum to draw the exhaust through the filter.

Filter to TEM

As the thermophoresis method did not work after the denuder, the authors decided to remove soot from the filter and prepare for TEM imaging. To remove the soot from the filter for TEM imaging, a small sample of the quartz filter was peeled away. The quartz filters are easy to break apart and a top layer, containing the soot collected was quite easy to remove. A small section of the top was soaked in around 3 ml of ethanol in a small glass petri dish. With adequate agitation, much of the soot lifted from the quartz and was dispersed in the ethanol. This soot laden ethanol was then moved to a small sample bottle and further diluted with approx. 2ml of ethanol. A number of strategies were then tested. A sample was subjected to sonication by placing the sample bottle in an ultrasonic bath, for around 1 hour. Another sample was sonicated for 5 minutes using an ultrasonic mixing probe at 20W, 3mm probe, 50% duty cycle (Hielscher UP200Ht). These samples were then left for 5 days. Over the 5 days, any quartz fibres present had dropped to the bottom of the sample bottle. Some sample was drawn from the bottle and diluted into another sample bottle. This was then subjected to another round of sonication. Drops of these samples were then pipetted onto the TEM grids. The ethanol evaporates and a dispersed soot sample is left on the grid.

It was found that the second sonication stage was important to ensure any entangled soot aggregates formed during the filter sedimentation phase were broken apart and that all sizes were well dispersed in the ethanol. It was also found that the drops added to the grid were best done immediately after the second sonication stage. If adequate sonication was not done or the period between sonication and dropping onto the grid was too long, large cluster of agglomerates were visible in the TEM images (Figure 10) leading to a skew of the data to larger sizes when post processing was conducted. The ultrasonic probe resulted in better dispersion than the ultrasonic bath and was used for the results reported here.

TEM imaging

For analysis and imaging three grids were examined,

1. Soot sampled in the exhaust using the thermophoresis probe, (no denuder-direct).
2. Soot sampled from exhaust, no denuder, onto filter then washed off (no denuder-filter wash).
3. Soot sampled from exhaust, through the denuder, onto filter then washed off (denuder-filter wash).

Collection of the soot for TEM analysis from the exhaust using the direct to grid and the filter method provides a comparison to access if the filter wash technique resulted in any changes to the soot imaged and help validate the methodology and preparation. The soot on the grids was the imaged in a JEOL JEM-2100F, operated at 200kV with a Gatan Ultrascan 1000 camera. The applied magnification was set at 6000 for morphological measurements and 20,000 for the measurement of primary soot particles. For morphological analysis, 5 locations on each grid, with 10 images were taken at each location, as outlined in the work [27].

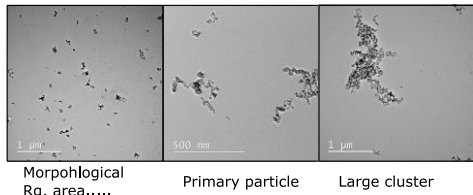


Figure 10. TEM images used for morphological measurement, and large cluster form under-sonication and bad grid prep.

Methods to post process and conduct morphological analysis is introduced in a number of previous works too numerous to recount here [10]. The analysis conducted here has been taken from the work [22], this represents a recent study conducted at the end of a review stage so contains up to date analysis methodologies. Image processing is conducted in Matlab using a script with minor modifications as the script used in [22]. The Matlab script detects and quantifies morphological parameters as defined in Figure 11.

Radius of gyration is a root mean square radius that quantifies the overall size of the aggregate and is determined using the distances of each pixel in a particle image from the pixel at the particle centroid of (2D):

$$R_g^2 = \frac{1}{m} \sum_{i=1}^m r_i^2 \quad (1)$$

R_g = Radius of gyration

m =number of pixels in aggregate

r_i = distance between pixel and the centroid of the aggregate

Fractal dimension (D_f) of a soot aggregate can be calculated using radius of gyration and other parameters

$$n = k_f \left[\frac{R_g}{d_p} \right]^{D_f} \quad (2)$$

where n is the number of primary particles in an aggregate and k_f is a fractal pre-factor, d_p is the average diameter of primary particles and is calculated from

$$n = \left[\frac{A}{A_p} \right]^\alpha \quad (3)$$

where A is the projected area of an aggregate and $\alpha=1.09$. A_p is the projected area of the average particle, determined from the average diameter of the primary particle. This was determined from measuring the primary particle size in aggregates using a separate Matlab script and the higher magnification images (20,000), between 140 and 300 primary particles were measured. Fractal dimension is calculated as the slope of a linear regression of $\ln(n)$ vs $\ln(R_g/d_p)$. An increase in D_f means more compact, clustered soot aggregates, a lower D_f means more stretched, chain-like aggregate structures. The projected area equivalent diameter, D_a was also determined. D_a has been shown in previous [9] work to be comparable to mobility diameters (mobility diameter is the classification of size separation used by the DMS).

The distribution of the diameter of gyration ($D_g = R_g \times 2$) and the projected area equivalent diameter are shown Figure 12 for the three cases. For each sample, the number of agglomerates processed from the 50 images used was;

No denuder direct= 1641 particle agglomerates

No denuder from filter= 1390 particle agglomerates

Denuder from filter= 1687 particle agglomerates

Page 6 of 9

06.06.2019

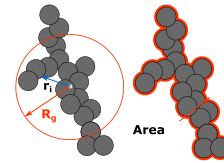


Figure 11. Soot morphological scheme.

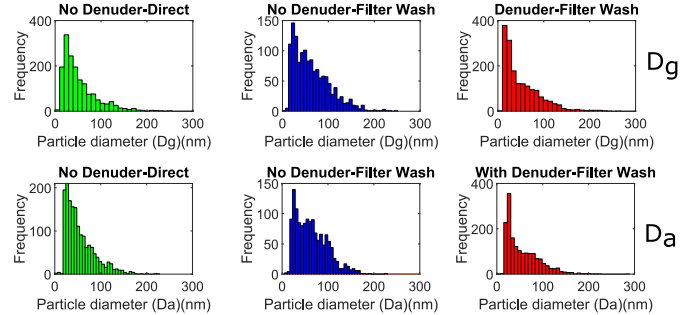


Figure 12. Distribution of D_g and D_a .

The distribution of the primary particle diameters for each sample is shown in Figure 13. Using the d_p with Eqn. (3) and (2) the fractal dimension for the each sample has been determined and is also shown in Figure 13. The fractal dimensions of the samples are in good agreement between the sampling techniques. The filter wash method has a slightly larger fractal dimension compared to the direct to grid method, suggesting the wash method has compacted the particles somewhat. This would need to be validated with several repeats of this imaging to confirm this is in fact a true morphological effect, not a limit of the imaging, post processing and limited number of particles imaged.

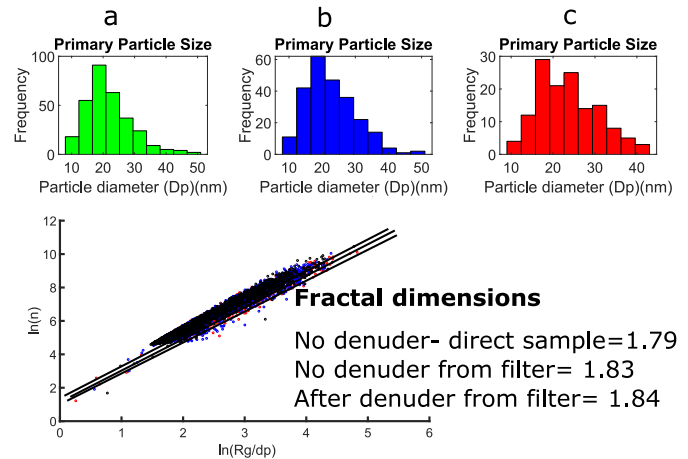


Figure 13. d_p distribution along with $\ln(n)$ vs $\ln(R_g/d_p)$ plot to determine fractal dimension.

The TEM and the DMS results are brought together in Figure 14. The TEM results from the three samples: No denuder direct, no denuder filter wash and denuder filter wash show a generally good correlation between themselves for all measures. For the D_a the peak for all cases is at the same size, D_g peak is close to being the same. The small differences in distribution between the samples is too small to suggest any systematic difference due to the nature of the soot. To really examine this, more grids would need to be sampled. The fact that the samples from the filter wash and those from direct to grid (using the

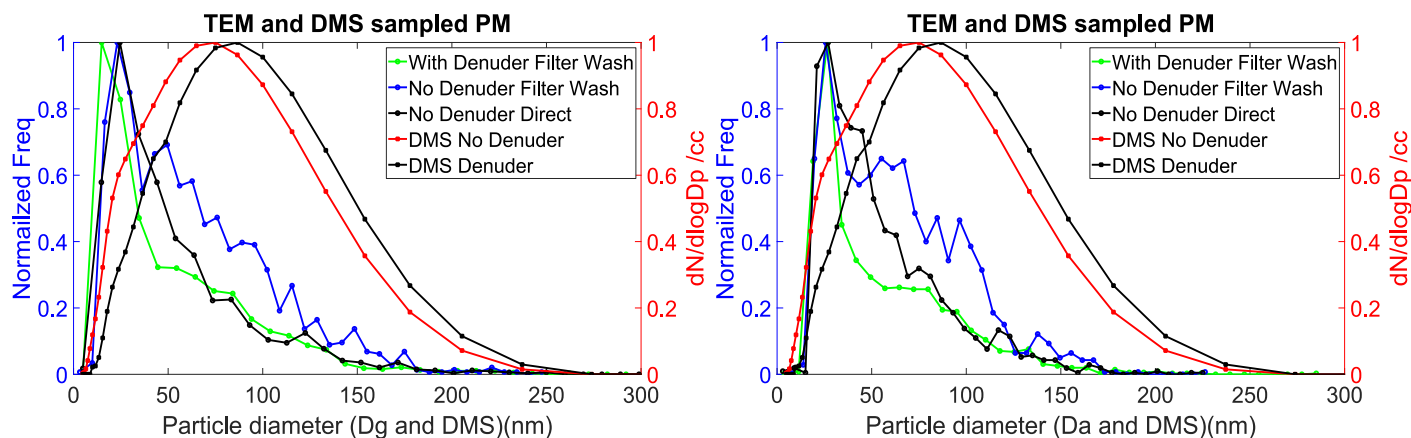


Figure 14 Dg and Da distributions, plotted with normalized DMS results, with and without the denuder. Da and Dg from direct and filter collected soot.

probe) are very similar suggests that sampling direct onto the grid in the exhaust and using the quartz filters, with the proper grid preparation are equivalent. From the TEM results there is no impact on soot morphological data from the denuder.

The distribution of both the D_g and the D_a never match that of the DMS measurement. It is important to remember that the D_g and the mobility diameter (D_m) that the DMS measures are not the same thing-however: some equivalence or similarity in distribution was expected, particularly with D_a , considering the work [9, 28]. The relationship between the two is complex, depending on the primary particle size, number of primary particles in each aggregate, the fractal dimension and the Knudsen number regime, Kn , the ratio of molecular mean free path (gas) to the particle size, $Kn \ll 1$ continuum regime, as we have here. The work [28] suggests $D_m/D_g = 1.3$ to 0.75 for diffusion limited cluster aggregation (DLCA) in the continuum regime. This rescaling between the classes would not alter the discrepancy in size distribution observed here. The lack of similarity between DMS and TEM size distributions cannot be explained so far, the 2D nature of a TEM image and the 3D nature of the DMS measurement is postulated to be a factor, but is unlikely to account for discrepancy completely. More work is proposed to examine the soot from different rings of column in the DMS and image the soot of defined D_m .

TGA Procedure

A TGA was conducted as an indicator of VOC content of the soot, before and after the denuder. Approx. 2mg of soot for TGA analysis could be collected after 30mins. Soot for the TGA was prepared by peeling off the upper, soot laden layer of the filter and then grinding this sample in a small mortar in pestle. This sample was stored in a cabinet complete with drier to avoid any water condensing into the sample. The powder sample was then easily placed on the small platinum trays for the TGA.

A quartz filter was broken up and ground for TGA analysis with no soot, this was done to check that the filters were in fact inert in the TGA. The filter was heated in an oxidation environment, up to 700°C for one hour with no significant mass change. The soot samples were tested in the TGA according to the procedure outlined in Table 1. Stage 0-5 are to determine the volatile fraction, stage 6-7 are to prepare the oxidative stage and stage 8-9 are the oxidation of the soot.

Table 1 TGA procedure

Stage	Description
0	Samples are in Nitrogen
1	Ramp $10^\circ\text{C}/\text{min}$ to 30°C
2	Isothermal for 30 min (to stabilize the sample)
3	Ramp $10^\circ\text{C}/\text{min}$ to 550°C
4	Isothermal for 60 min (to remove volatile matter)
5	Ramp $10^\circ\text{C}/\text{min}$ to 700°C (check to remove all volatiles)
6	Cool to 30°C
7	Introduce air
8	Ramp $10^\circ\text{C}/\text{min}$ to 700°C (oxidation)
9	Isothermal for 60 min

The normalized mass reduction in the TGA is shown in Figure 15. Soot consists of heavier hydrocarbons which have condensed onto the surface, the sample is heated in nitrogen, the volatile organic fraction (VOF) of the soot evaporates. The volatile organics tend to fill the porous surface of the soot. At lower exhaust temperatures, such as those observed with the lower speed, lower load conditions previously examined (Figure 2) the VOF may tend to form nucleation particle as well as absorbing onto the soot. The sample that has been through the denuder would be expected to have a lower VOF as the denuder has evaporated and absorbed most of the VOCs which would form the VOF of the soot hence; the sample that had been collected after the denuder would ideally show almost no mass change during the devolatilization (devol) phase. Soot sampled with no denuder will contain the maximum VOF (for this condition). Figure 15 shows that the no-denuder sample experienced a mass loss of approx. 3.75% during the devol phase, the sample that had gone through the denuder experienced a mass loss of approx. 2.75%. For each sample, the TGA result includes a mixture of soot with volatiles and quartz fibres, which would make up a considerable amount of the total mass present in the sample, these would remain unchanged during the heating phases. The rate of change of mass is greater for the no-denuder sample during the shaded period of stage 3 (Figure 15). This corresponds to the period in the TGA up to approx. 300°C , the temperature that the denuder operates at, hence the denuder has removed some of the VOC in the 300°C evaporation range but has not been effective at removing all of them. This may be due to the residence time in the heater or re-

condensing of those VOCs in cooler parts of the denuder, back onto the soot surface.

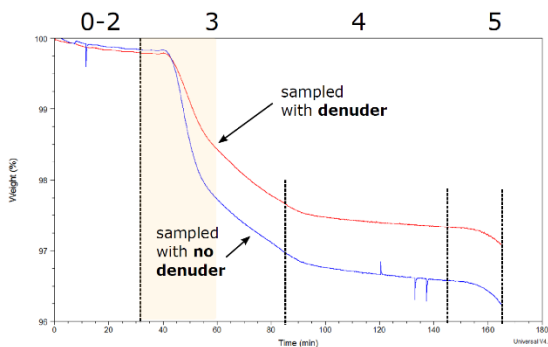


Figure 15. Normalized mass loss from TGA during devolatilization.

Above 300°C, the devol TGA shows a similar rate for both samples, suggesting the denuder has been ineffective at removing the heavier hydrocarbon. Both samples underwent extremely similar oxidation in the TGA, suggesting the denuder had no effect on the reactivity of the soot sampled, Figure 16.

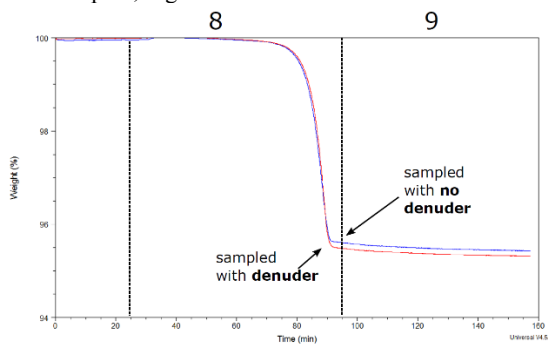


Figure 16. Normalized mass loss from TGA during oxidation.

Summary and Conclusion

Soot has been sampled from an instrumented engine using a differential mobility spectrometer (DMS 500) and collected for imaging in a TEM. To examine the effect of volatiles and to try and compare the DMS and the TEM sizing of the soot, a thermal denuder was built and used, in accordance with previous works. In using the denuder, an alternative collection method for the TEM needed to be used. A cooled glass surface was tried as a soot collection tool. This method did not work. A quartz filter was then used with sample preparation involving washing in ethanol and sonication for TEM imaging. Soot from the filter was also used to conduct a TGA to investigate effectiveness of the denuder. The collection methods used, direct to grid and filter wash, were equivalent to each other in terms of distribution of sizes. A small difference in fractal dimension was observed between the techniques, which would need further testing to substantiate a systematic difference between the techniques.

Generally, the thermal denuder performed poorly, making DMS measurement difficult to examine due to uncertainty of sample loss. The TGA results suggest that the denuder removed some of the volatiles in boiling range up to 300°C but not all.

The overall aim to compare TEM and DMS measurements has only been semi successful. Whilst the full range of techniques applied to

conduct sampling and measurement have been applied diligently the TEM and DMS distributions are not similar. The relationship between the D_m that the DMS measurements and the D_g and D_a that has been measured in the TEM needs to be further investigated. The aim of developing a robust test protocol has been met, with special attention to the correlation between direct to grid and filter wash techniques. The thermal denuder is most likely not to be used in its current form in future testing.

References

- Burtscher, H., Physical characterization of particulate emissions from diesel engines: a review. *Journal of Aerosol Science*, 2005. 36(7): p. 896-932.
- Kittelson, D.B., Engines and nanoparticles: a review. *Journal of Aerosol Science*, 1998. 29(5): p. 575-588.
- Giechaskiel, B., et al., Review of motor vehicle particulate emissions sampling and measurement: From smoke and filter mass to particle number. *Journal of Aerosol Science*, 2014. 67: p. 48-86.
- Kittelson, D.B., et al., Driving Down On-Highway Particulate Emissions. 2006, SAE International.
- Zheng, Z., et al., Investigation of solid particle number measurement: Existence and nature of sub-23nm particles under PMP methodology. *Journal of Aerosol Science*, 2011. 42(12): p. 883-897.
- Symonds, J.P.R., et al., Diesel soot mass calculation in real-time with a differential mobility spectrometer. *Journal of Aerosol Science*, 2007. 38(1): p. 52-68.
- Reavell, K., T. Hands, and N. Collings, A Fast Response Particulate Spectrometer for Combustion Aerosols. 2002, SAE International.
- Zhang, Y., et al., The soot particle formation process inside the piston bowl of a small-bore diesel engine. *Combustion and Flame*, 2017. 185: p. 278-291.
- Park, K., D.B. Kittelson, and P.H. McMurry, Structural Properties of Diesel Exhaust Particles Measured by Transmission Electron Microscopy (TEM): Relationships to Particle Mass and Mobility. *Aerosol Science and Technology*, 2004. 38(9): p. 881-889.
- Ouf, F.X., et al., Influence of Sampling and Storage Protocol on Fractal Morphology of Soot Studied by Transmission Electron Microscopy. *Aerosol Science and Technology*, 2010. 44(11): p. 1005-1017.
- Van Gulijk, C., et al., Measuring diesel soot with a scanning mobility particle sizer and an electrical low-pressure impactor: performance assessment with a model for fractal-like agglomerates. *Journal of Aerosol Science*, 2004. 35(5): p. 633-655.
- Wang, Y., et al., Effect of lubricant oil additive on size distribution, morphology, and nanostructure of diesel particulate matter. *Applied Energy*, 2014. 130: p. 33-40.
- Miyashita, K., et al., TEM Analysis of Soot Particles Sampled from Gasoline Direct Injection Engine Exhaust at Different Fuel Injection Timings. 2015, SAE International.
- Seong, H., et al., Characterization of Particulate Morphology, Nanostructures, and Sizes in Low-Temperature Combustion with Biofuels. 2012, SAE International.
- Amanatidis, S., et al., Comparative performance of a thermal denuder and a catalytic stripper in sampling laboratory and marine exhaust aerosols. *Aerosol Science and Technology*, 2018. 52(4): p. 420-432.

16. Armas, O., K. Yehliu, and A.L. Boehman, Effect of alternative fuels on exhaust emissions during diesel engine operation with matched combustion phasing. *Fuel*, 2010. 89(2): p. 438-456.
17. Kirchner, U., et al., TEM study on volatility and potential presence of solid cores in nucleation mode particles from diesel powered passenger cars. *Journal of Aerosol Science*, 2009. 40(1): p. 55-64.
18. Kittelson, D.B., et al., On-Road Exposure to Highway Aerosols. 1. Aerosol and Gas Measurements. *Inhalation Toxicology*, 2004. 16(sup1): p. 31-39.
19. Burtcher, H., et al., Separation of volatile and non-volatile aerosol fractions by thermodesorption: instrumental development and applications. *Journal of Aerosol Science*, 2001. 32(4): p. 427-442.
20. Stevanovic, S., et al., Characterisation of a Commercially Available Thermodesorber and Diffusion Drier for Ultrafine Particles Losses. *Aerosol and Air Quality Research*, 2015. 15(1): p. 357-363.
21. Wehner, B., S. Philippin, and A. Wiedensohler, Design and calibration of a thermodesorber with an improved heating unit to measure the size-dependent volatile fraction of aerosol particles. *Journal of Aerosol Science*, 2002. 33(7): p. 1087-1093.
22. Rohani, B. and C. Bae, Morphology and nano-structure of soot in diesel spray and in engine exhaust. *Fuel*, 2017. 203: p. 47-56.
23. Emberson, D.R., Arctic Biodiesel Performance and PM Number Emissions, in *The Ninth International Conference on Modeling and Diagnostics for Advanced Engine Systems (COMODIA 2017)*. 2017: Okayama, Japan.
24. Rohani, B. and C. Bae, Effect of exhaust gas recirculation (EGR) and multiple injections on diesel soot nano-structure and reactivity. *Applied Thermal Engineering*, 2017. 116: p. 160-169.
25. Yehliu, K., et al., Impacts of advanced diesel combustion operation on soot nanostructure and reactivity. *International Journal of Engine Research*, 2016. 18(5-6): p. 532-542.
26. Song, J., et al., Examination of the oxidation behavior of biodiesel soot. *Combustion and Flame*, 2006. 146(4): p. 589-604.
27. Kondo, K., et al., Uncertainty in Sampling and TEM Analysis of Soot Particles in Diesel Spray Flame. 2013, SAE International.
28. Sorensen, C.M., *The Mobility of Fractal Aggregates: A Review*. *Aerosol Science and Technology*, 2011. 45(7): p. 765-779.

Contact Information

David Emberson
 david.r.emberson@ntnu.no

Acknowledgments

The authors would like to acknowledge support from the Research Council of Norway through the Norwegian Center for Transmission Electron Microscopy, NORTEM (197405/F50)